3330–3345 *Nucleic Acids Research, 2014, Vol. 42, No. 5* *Published online 24 December 2013*
doi:10.1093/nar/gkt1337

The *Dictyostelium discoideum* RNA-dependent RNA polymerase RrpC silences the centromeric retrotransposon DIRS-1 post-transcriptionally and is required for the spreading of RNA silencing signals

Stephan Wiegand[1], Doreen Meier[2], Carsten Seehafer[1], Marek Malicki[1], Patrick Hofmann[1], Anika Schmith[3], Thomas Winckler[3], Balint Földesi[2], Benjamin Boesler[2], Wolfgang Nellen[2], Johan Reimegård[4], Max Käller[4], Jimmie Hällman[4], Olof Emanuelsson[4], Lotta Avesson[5], Fredrik Söderbom[6,7] and Christian Hammann[1,*]

[1]Ribogenetics@Biochemistry Lab, School of Engineering and Science, Molecular Life Sciences Research Center, Jacobs University Bremen, Campus Ring 1, DE-28759 Bremen, Germany, [2]Abteilung Genetik, Universität Kassel, Heinrich-Plett-Strasse 40, DE-34132 Kassel, Germany, [3]Friedrich-Schiller-Universität Jena, Institut für Pharmazie, Lehrstuhl für Pharmazeutische Biologie, Semmelweisstraße 10, DE-07743 Jena, Germany, [4]Division of Gene Technology, KTH Royal Institute of Technology, Science for Life Laboratory (SciLifeLab Stockholm), School of Biotechnology, SE-171 65 Solna, Sweden, [5]Garvan Institute of Medical Research, 384 Victoria St Darlinghurst, NSW 2010, Australia, [6]Department of Cell and Molecular Biology, Biomedical Center, Uppsala University, PO Box 596, S-75124 Uppsala, Sweden and [7]Science for Life Laboratory, SE-75124 Uppsala, Sweden

Received August 6, 2013; Revised November 29, 2013; Accepted November 30, 2013

ABSTRACT

Dictyostelium intermediate repeat sequence 1 (DIRS-1) is the founding member of a poorly characterized class of retrotransposable elements that contain inverse long terminal repeats and tyrosine recombinase instead of DDE-type integrase enzymes. In *Dictyostelium discoideum*, DIRS-1 forms clusters that adopt the function of centromeres, rendering tight retrotransposition control critical to maintaining chromosome integrity. We report that in deletion strains of the RNA-dependent RNA polymerase RrpC, full-length and shorter DIRS-1 messenger RNAs are strongly enriched. Shorter versions of a hitherto unknown long non-coding RNA in DIRS-1 antisense orientation are also enriched in *rrpC*$^{-}$ strains. Concurrent with the accumulation of long transcripts, the vast majority of small (21 mer) DIRS-1 RNAs vanish in *rrpC*$^{-}$ strains. RNASeq reveals an asymmetric distribution of the DIRS-1 small RNAs, both along DIRS-1 and with respect to sense and antisense orientation. We show that RrpC is required for post-transcriptional DIRS-1 silencing and also for spreading of RNA silencing signals. Finally, DIRS-1 mis-regulation in the absence of RrpC leads to retrotransposon mobilization. In summary, our data reveal RrpC as a key player in the silencing of centromeric retrotransposon DIRS-1. RrpC acts at the post-transcriptional level and is involved in spreading of RNA silencing signals, both in the 5′ and 3′ directions.

INTRODUCTION

Cellular RNA-dependent RNA Ppolymerases (RdRPs) are present in many eukaryotic organisms, including mammals (1), are involved in mechanisms of RNA-mediated gene regulation including RNA interference (RNAi) (2,3). RdRPs synthesize an RNA strand from a complementary RNA template, leading to either long or small antisense transcripts. Based on *in vivo* and *in vitro* studies, including deep sequencing analyses, several primer-dependent and -independent modes of action have been inferred for RdRPs from different organisms. These frequently lead to an amplification of a primary silencing signal such as double-strand-derived small interfering RNA (siRNA). An amplifying component

*To whom correspondence should be addressed. Tel: +49 4212 003 247; Fax: +49 4212 003 249; Email: c.hammann@jacobs-university.de

was postulated by Fire and Mello when they first described RNAi in *Caenorhabditis elegans* (4), leading to the identification of RdRP EGO-1 as the responsible enzyme (5). When RNA was injected against a reporter gene, secondary siRNAs were observed that predominantly localize 5′ of the original trigger, and this 5′ spreading was shown to be RdRP-dependent (6). This phenomenon, known as 'transitivity', is diagnostic for RdRP activity *in vivo* (6–8). We recently observed transitivity in the amoeba *Dictyostelium discoideum*, and have shown that it depends on the presence of the RdRP RrpC and the dicer-related nuclease DrnB, as inferred from an artificial reporter system (9). RrpC is one of three RdRPs in *D. discoideum*, all of which show a similar domain structure (Supplementary Figure S1) (10).

Dictyostelium intermediate repeat sequence 1 (DIRS-1) is the founding member of a poorly characterized class of long terminal repeat (LTR) retrotransposons. DIRS elements differ from other LTR retrotransposons by having inverted instead of direct terminal repeats, lacking an aspartic protease domain and using a tyrosine recombinase instead of a DDE-type integrase protein for integration. Thus, DIRS elements use a retrotransposition mechanism fundamentally different from that of other LTR retrotransposons [reviewed in (11)]. This may favor the recombinatorial integration into preexisting copies of the same element as seen in the *D. discoideum* genome. The genome of *D. discoideum* features ~40 intact copies and ~200–300 fragments of DIRS-1, which thus represents the most frequently occurring LTR retrotransposon in the amoeba (12). DIRS-1 sequences accumulate at one end of each chromosome (12), and these clusters have been suggested to represent the centromeres of the chromosomes in *D. discoideum* (13,14). Although observed clustering of DIRS-1 elements may result from preferential integration of mobilized DIRS-1 copies into preexisting DIRS-1 clusters (15), it is not known whether the apparent clustering of these elements is the result of deleterious integration into coding regions of the haploid *D. discoideum* genome that removes affected cells from the population (16). Nonetheless, uncontrolled amplification of DIRS-1 elements and integration into centromeric regions may seriously compromise centromere stability, and thus genome integrity.

DIRS-1 is transcribed as a 4.5-kb-long messenger RNA (mRNA) with three overlapping open reading frames (ORFs) (Figure 1A) (17). The left LTR possesses promoter activity to drive the transcription of the DIRS-1 mRNA (18). These DIRS-1 mRNA transcripts were found to accumulate during *D. discoideum* development and contain parts of the two LTRs (18). Additionally, heat shock or other stress conditions can trigger the expression of a 900-nt-long antisense transcript (Figure 1A), which, however, is not expressed under the axenic growth conditions applied in this study (19,20).

For retrotransposition to occur, the mRNA is thought to be reverse transcribed by the enzyme activity of ORF III (17). The ends of the resulting linear complementary DNA (cDNA) feature the LTR fragments, which exhibit sequence complementarity to a DIRS-1 region termed the internal complementary region (ICR). According to a model put forward by Lodish *et al*. the ICR serves to bring the 5′- and the 3′-end of the reverse transcript together (11) to generate a single-stranded circular DNA replication intermediate that serves as template for the generation of a double-stranded circular DNA to be inserted in the genome (17).

We have shown earlier that the LTR of DIRS-1 is methylated by the sole DNA methyltransferase, DnmA, identified in *D. discoideum* (21). Surprisingly, no transcriptional activation was observed in a *dnmA* gene deletion strain, indicating that DIRS-1 is not under transcriptional control, at least not by DnmA. However, in that study, we observed that regulation of DIRS-1 expression may be controlled at the post-transcriptional level involving small RNAs (21). Here, we show that RrpC controls DIRS-1 post-transcriptionally, and its activity is required to prevent DIRS-1 retrotransposition. We further report RrpC-dependent spreading of an RNA silencing signal in the 3′ direction in *D. discoideum*.

MATERIALS AND METHODS

Oligonucleotides

DNA oligonucleotides (Sigma) used in this study are listed in Supplementary Table S1.

Genes and strains

All experiments were carried out with AX2 and derivatives. All *D. discoideum* strains were grown axenically in HL5 medium. The *rrp* genes are listed in the online resource dictybase.org with their accession numbers DDB_G0289659 (*rrpA*), DDB_G0291249 (*rrpB*) and DDB_G0280963 (*rrpC*), and the generation of their single and multiple deletion strains was described recently (9). The *trx-1* gene has the accession number DDB_G0294447.

RNA isolation

Total RNA was isolated from 5×10^7 cells of axenically grown *D. discoideum* strains using TRIzol® (Invitrogen). Cells were pelleted for 5 min at 500 rcf/4°C and washed in 20 ml pre-cooled Sorenson phosphate buffer (2 mM Na_2HPO_4, 15 mM KH_2PO_4, pH 6.0, with H_3PO_4). On re-centrifugation of cells under the same conditions, they were lysed in 1 ml of TRIzol® reagent for 5 min. On addition of 200 µl of chloroform, the material was vortexed and incubated for 3 min at room temperature. Phases were separated by centrifugation at 16 000 rcf/4°C for 20 min. RNA was precipitated by addition of equal amounts of 100% isopropanol, incubation for 10 min at room temperature and centrifugation at 16 000 rcf/4°C for 15 min. On washing twice with 70% ethanol, the pellet was dried and re-suspended in 150 µl dH_2O. RNA concentration was determined using a NanoDrop spectrophotometer (Peqlab).

Northern blotting

For total RNA blots, 10 µg was separated by gel electrophoresis in a 1.2% GTC-agarose gel in 1 × Tris

borate + ethylenediaminetetraacetic acid (pH 8.2). On capillary transfer to nylon membranes (Roti®-Nylon plus), ultraviolet cross-linking was carried out (0.5 J/cm^2). Prehybridization and hybridization were carried out in Church buffer [500 mM sodium phosphate (pH 7.2), 1 mM ethylenediaminetetraacetic acid, 7% w/v sodium dodecyl sulphate (SDS), 1% w/v bovine serum albumin] using radioactively labeled *in vitro* transcripts or polymerase chain reaction (PCR) products. Hybridization conditions are summarized in Supplementary Tables S2 and S3. All blots were washed twice for 15 min in 2 × saline sodium citrate (SSC), 0.1% w/v SDS, twice for 10 min in 1 × SSC, 0.1% w/v SDS and twice for 5 min in 0.5 × SSC, 0.1% w/v SDS. As control, blots were hybridized on stripping to probes against actin6 mRNA.

For small RNA blotting, 20μg total RNA was separated by gel electrophoresis in a 11% polyacrylamide gel in 20 mM MOPS (pH 7.0). On electroblotting onto a nylon membrane (Amersham Hybond^{TM}-NX) for 10 min at 20 V in dH_2O (semi-dry), RNA was chemically cross-linked as described recently (22). Small RNAs were probed with 5′ radioactively labeled DNA oligonucleotides as summarized in Supplementary Table S4. All other procedures were carried out as described for ultraviolet cross-linking, except for the use of the small nucleolar RNA (snoRNA) DdR-6 as loading control.

Southern blotting

Isolation of genomic DNA from 1–2 × 10^8 *Dictyostelium* cells for Southern blotting (23) was performed as described (24). For DNA digestion with restriction enzymes, aliquots containing 20 μg of DNA were incubated with *Sac* I, *Kpn* I or *Eco* RI (20 U/10 μg of DNA). After precipitation, samples were separated on 1.2% agarose gels for 14 h at a field strength of 1.5 V/cm, and fragments were visualized by ethidium bromide staining (0.5 μg/ml) for 30 min. DNA was denatured by soaking the gel in 10 volumes of denaturation buffer (1.5 M NaCl, 0.5 M NaOH) for 45 min, followed by 45 min soaking in neutralization buffer (3 M NaCl, 0.5 M Tris-HCl, pH 7). DNA fragments were transferred to a nylon membrane as described (25). Cross-linking and hybridization were carried out as described for northern blotting, using the right element sequence, labeled with [α-^{32}P]dATP by random priming. On overnight incubation, the membrane was washed with 3 × SSC, 0.01% SDS and then with 0.1 x SSC, 0.1% SDS, each at 60°C and for 1 h.

Generation of expression constructs

pTX-DIRS-1rLTRfw-GFP was generated by initially digesting the original vector pTX-GFP (26) with *Sal* I and ligating the oligonucleotides pTX-MCS-fw and pTX-MCS-rev for generating a multiple cloning site (MCS). Depending on the orientation of the MCS, the resulting vectors were termed pTX-MCSfw-A15-GFP and pTX-MCSrev-A15-GFP. To insert the DIRS-1 rLTR-sequence, plasmid pGEM®-T Easy DIRS-1 rLTR (21) was digested with *Sac* II and *Sal* I. Ligation into the MCS of pTX-MCSfw-A15-GFP and pTX-MCSrev-A15-GFP yielded the plasmids pTX-DIRS-1rLTRfw-A15-GFP and pTX-DIRS-1rLTRrev-A15-GFP. The former was digested with *Sac* II and *Xho* I to isolate the expression cassette, which was ligated into the vector pLPBLP (27), that had been digested with the same enzymes beforehand. From this, the Actin15-promoter was removed by a restriction digest with *Hin*d III and *Xho* I. The 5′ overhangs were filled by Klenow fragment before ligation, and the expression cassettes without Actin15-promoter were ligated back in the original vector using a *Sac* II and *Xho* I, which yielded the plasmid pTX-DIRS-1rLTRfw-GFP. From pTX-DIRS-1rLTRrev-A15-GFP, the expression cassette was removed with *Sal* I and *Bam*H I and ligated into the vector pJET1-H2Bv1, from which the H2Bv1 fragment had been removed with the same enzymes. The actin15-promoter was removed by a digest with *Hin*d III and *Sac* II, and the vector was re-ligated on removal of 5′ overhangs using Klenow fragment. The expression cassette was back-cloned into the original vector using *Sal* I and *Bam*H I, yielding plasmid pTX-DIRS-1rLTRrev-GFP.

The DIRS-1 ORFs were amplified by PCR using primers listed in Supplementary Table S1. PCR products were ligated into the cloning pJET1.2/blunt, and the resulting plasmids were sequenced. The ORF DNAs were excised by means of *Bam*H I and *Spe* I digests and ligated into pDM323 (28) that was previously linearized with *Bgl* II and *Spe* I. The resulting plasmids were transformed in AX2 and rrpC knockout strains, and transformation populations were used for further experiments. For the GFP-alone control, plasmid pDM317 (28) was used that features an ATG in front of the GFP coding sequence, allowing to monitor GFP expression by western blotting.

Fluorescence *in situ* hybridization and microscopy

Fluorescence *in situ* hybridization (FISH), using digoxigenin-labeled dNTPs, and 4,6-diamidino-2-phenylindole (DAPI) staining were performed as described recently (29). For the generation of probes for FISH, oligonucleotides DIRS1 forward and DIRS1 reverse were used, resulting in a 503-nt-long single-stranded DNA of DIRS-1 sense or antisense orientation, depending on their relative concentration in asymmetric PCRs. The fragment begins at the left end (LE) of ORF III (Figure 1) and is extended by 200 nt. Pictures were generated using an Alexa Fluor 488-coupled secondary antibody.

Quantitative real-time PCR

Expression analysis by quantitative real-time PCR (qRT-PCR) was carried out as described recently (30,31). In brief, total RNA was isolated using the Qiagen RNeasy Mini kit according to the provided protocol from 2 × 10^7 cells that were collected from exponentially growing cells and frozen at −80°C until further use. cDNA was synthesized by reverse transcription of 500 ng of total RNA using an oligodeoxythymidine primer and the Qiagen Omniscript RT kit. The Q1 and Q2 fragments of DIRS-1 were amplified from oligo(dT)-primed cDNA

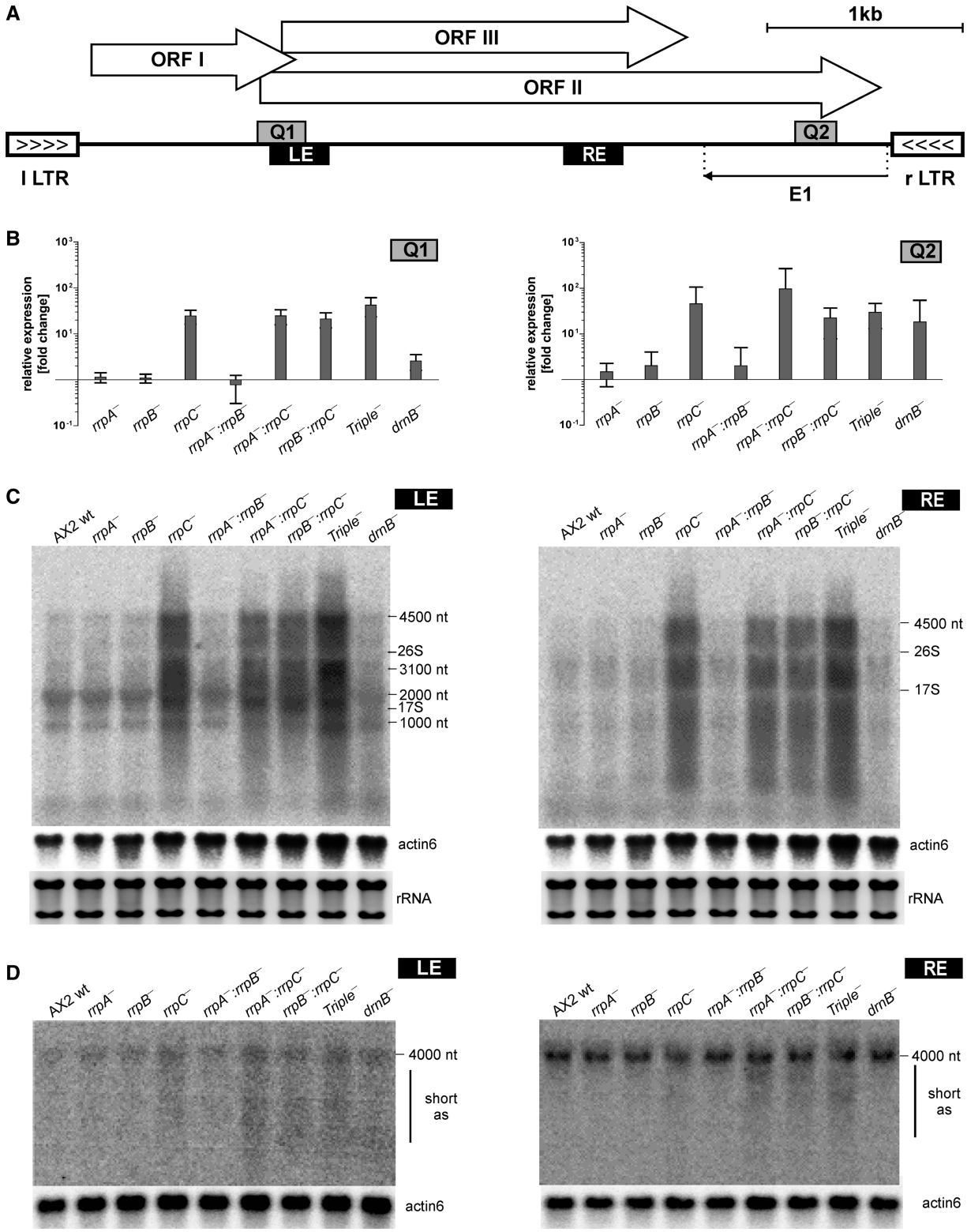

Figure 1. DIRS-1 expression. (**A**) Schematic representation of the DIRS-1 retrotransposon with the left and right inverted LTRs (l LTR and r LTR, respectively). The three ORFs, encoding the GAG protein (ORF I), the tyrosine recombinase (ORF II) and reverse transcriptase/RNase H domain and a methyltransferase (ORF III) are displayed together with the 900-nt E1 antisense transcript. Positions for expression analysis are Q1 and Q2 for qRT-PCR and LE and RE for northern blots. (**B**) Expression of DIRS-1 sequences in the indicated gene deletion strains, relative to the AX2 wild-type, as monitored by qRT-PCR using primer pairs at positions Q1 and Q2, and normalized to GAPDH expression. (**C**) Northern blot analysis of RNA from the indicated strains, using DIRS-1 sense strand-specific probes at positions LE (left) and RE (right). Ethidium bromide-stained rRNA served as loading control, while in northern blots, an actin6 probe acted to monitor transfer efficiency. (**D**) Northern blots using DIRS-1 antisense strand-specific probes at positions LE (left) and RE (right). Other details are as in (C). Size ranges of signals for shorter antisense RNAs are indicated to the right of each blot. Northern blot conditions are listed in Supplementary Tables S2 and S3. See also Figures 2 and 3 and Supplementary Figure S2.

with primer pairs Q-DIRS-01/-02 and Q-DIRS-03/-04, respectively. Expression of DIRS-1 was standardized against expression of the GAPDH gene, which was amplified using primers Q-gpdA-01 and Q-gpdA-02. Real-time amplification was carried out on a Stratagene Mx3000P instrument in 25 µl reaction mixes containing 1 × Taq buffer, 0.2 mM deoxynucleoside triphosphates, 0.4 µM primers, 1 × ROX reference dye (Jena Bioscience, Germany), 1 × EvaGreen solution (Jena Bioscience, Germany), varying amount of cDNA and 1.25 U Taq polymerase (Jena Bioscience, Germany). After an initial denaturing step at 95°C for 10 min, the PCR was performed for 40 cycles at 95°C for 30 s, 58°C for 30 s and 72°C for 30 s. Regulation was calculated by the method of Pfaffl (32).

Deep sequencing and computational analysis

RNA was prepared and converted to cDNA, from which sequencing libraries were prepared and sequenced using the Illumina platform as described recently (33). Endogenous siRNA populations in the AX2 wild-type and *rrpC* knockout strains, each in two biological replicates, were sequenced after ligation of Illumina TruSeq small RNA adapters that allow cluster amplification on the flow cell surface. Adapter sequences were trimmed from the sequences using Cutadapt (34) with at least 3-nt overlap allowing for 10% mismatches. The trimmed reads were mapped against a reference using Bowtie2 (35). The reference was either the genome of *D. discoideum* strain AX4 (downloaded from http://dictybase.org/) or our own repeat sequence library containing simple repeats from Repbase (36) and consensus sequences of interspersed repeats including DIRS-1. The default setting was used when mapping to the genome reference, while a more sensitive setting was used when mapping to the repeat reference (-M 500 -N 1 -L 20 -R 3 -D 20 -i S,1,0.50). Read count per annotated region (http://dictybase.org/download/gff3/) was extracted with HTSeq (http://www-huber.embl.de/users/anders/HTSeq/doc/overview.html). The read distribution was visualized with the integrative genomics viewer (37).

RESULTS

Accumulation of DIRS-1 sense transcripts in the absence of the *rrpC* gene

In a previous study, we observed the accumulation of transcripts of the retrotransposon DIRS-1 in a gene disruption strain of the RdRP RrpC (21). To study the impact of RdRPs on DIRS-1 expression in *D. discoideum* in detail, we made use of a recently introduced series of strains (9), with the genes of the RdRPs in all possible combinations deleted by a one-step cloning strategy (38) that is based on the Cre-lox system (27). Unlike in the originally used gene disruption strains (21), both functional domains of each *rrp* gene (Supplementary Figure S1) were removed completely (9), resulting in three single, three double and one triple *rrp* gene deletion strain. In addition, DIRS-1 expression was monitored in a gene deletion strain of the dicer-related nuclease DrnB (*drnB*$^{-}$) (39). Analyses by qRT-PCR using the two primer sets Q1 and Q2 (Figure 1A) showed a 50–100-fold increase of DIRS-1 RNA in all *rrpC* gene deletion strains compared with the isogenic wild-type strain (Figure 1B). In the *drnB*$^{-}$ strain, a 5–10-fold increase in RNA levels was observed, depending on which primer set was used. To assess how these RNA molecules correspond to full-length DIRS-1 RNA, we next carried out northern blot analyses with riboprobes against the left-end (LE) and right-end (RE) positions in the DIRS-1 sense transcript that localize to the 5′-end or the 3′ part of ORF III, respectively (Figure 1A). As shown in Figure 1C, these analyses revealed a considerable increase of a 4.5-kb fragment corresponding to the size of the DIRS-1 full-length mRNA (18) for each *rrpC* gene deletion strain, while the transcript levels in the *drnB*$^{-}$ strain appear similar to that observed in the wild-type strain (Figure 1C). In the *rrpC*$^{-}$ strains, the DIRS-1 transcripts display strong size heterogeneity as indicated by the smear in the respective lanes of the northern blots (summarized in Table 1).

A long DIRS-1 antisense transcript

Considering that antisense transcripts are prevalent, particularly in mobile genetic elements (40,41), we also used riboprobes that bind to the same LE and RE positions (Figure 1A) on an antisense transcript. We observed an RNA transcript of 4 kb by either riboprobe (Figure 1D). The existence of this hitherto unknown antisense RNA was also confirmed independently by strand-specific qRT-PCR (Supplementary Figure S2). We termed this long non-coding RNA (lncRNA) *long antisense DIRS-1* (lasDIRS-1) to discriminate it from the 900-nt E1 antisense transcript that is produced on heat shock (19,20), but not under the axenic growth conditions used in this study. Unlike the situation seen for the DIRS-1 mRNA, the lasDIRS-1 lncRNA displays a discrete size, and its RNA levels appear to be identical in either gene deletion strain investigated here. Only in the *rrpC*$^{-}$ strains was a light smear below the full-length lasDIRS-1 RNA observed reproducibly, indicating size heterogeneity (Figure 1D and summarized in Table 1).

Promoter activity of the DIRS-1 right LTR

Because the sense transcript is derived from the promoter activity of the left LTR (18), it seemed plausible that the inversely oriented right LTR sequence might contain the promoter to drive lasDIRS-1 transcription. To test this hypothesis, we generated two constructs, which contained the right LTR in forward or reverse orientation in front of a GFP expression cassette, but lacked any further promoter sequence (Figure 2A). Fluorescence microscopy of strains transformed with these two constructs revealed GFP expression only for the construct with the forward-oriented right LTR (Figure 2B). The promoter activity of the right LTR of DIRS-1 was also independently confirmed by western blotting (Figure 2C). These data strongly suggest that the lasDIRS-1 transcript derives from the right LTR of the retrotransposon.

Table 1. Characteristics of rrp gene deletion strains

rrp gene deletion	Change in DIRS-1 transcripts levels			Spreading of small RNA signal	
	mRNA[a]	lasDIRS1[b]	Small RNAs[c]	In 5′ direction[d]	In 3′ direction[e]
rrpA¯	Unchanged	Unchanged	Unchanged	ı	ı
rrpB¯	Unchanged	Unchanged	Unchanged	ı	ı
rrpC¯	Strongly increased	Shorter versions increased	Strongly decreased	Not observed	Not observed
rrpA¯:*rrpB*¯	Unchanged	Unchanged	Unchanged	ı	n.d.[f]
rrpA¯:*rrpC*¯	Strongly increased	Shorter versions increased	Strongly decreased	Not observed	n.d.[f]
rrpB¯:*rrpC*¯	Strongly increased	Shorter versions increased	Strongly decreased	Not observed	n.d.[f]
rrpA¯:*rrpB*¯:*rrpC*¯ (*Triple*¯)	Strongly increased	Shorter versions increased	Decreased	Not observed	n.d.[f]

[a]Relative to AX2 wild-type, as determined by qRT-PCR and northern blotting (Figure 1), [b]Relative to AX2 wild-type, as determined by qRT-PCR and northern blotting (Figure 1), [c]Relative to AX2 wild-type, as determined by northern blotting (Figure 4), [d]Shown in an earlier study using a β-galactosidase reporter assay (9), [e]As determined by northern blotting (Figure 6).
f n.d., not determined.

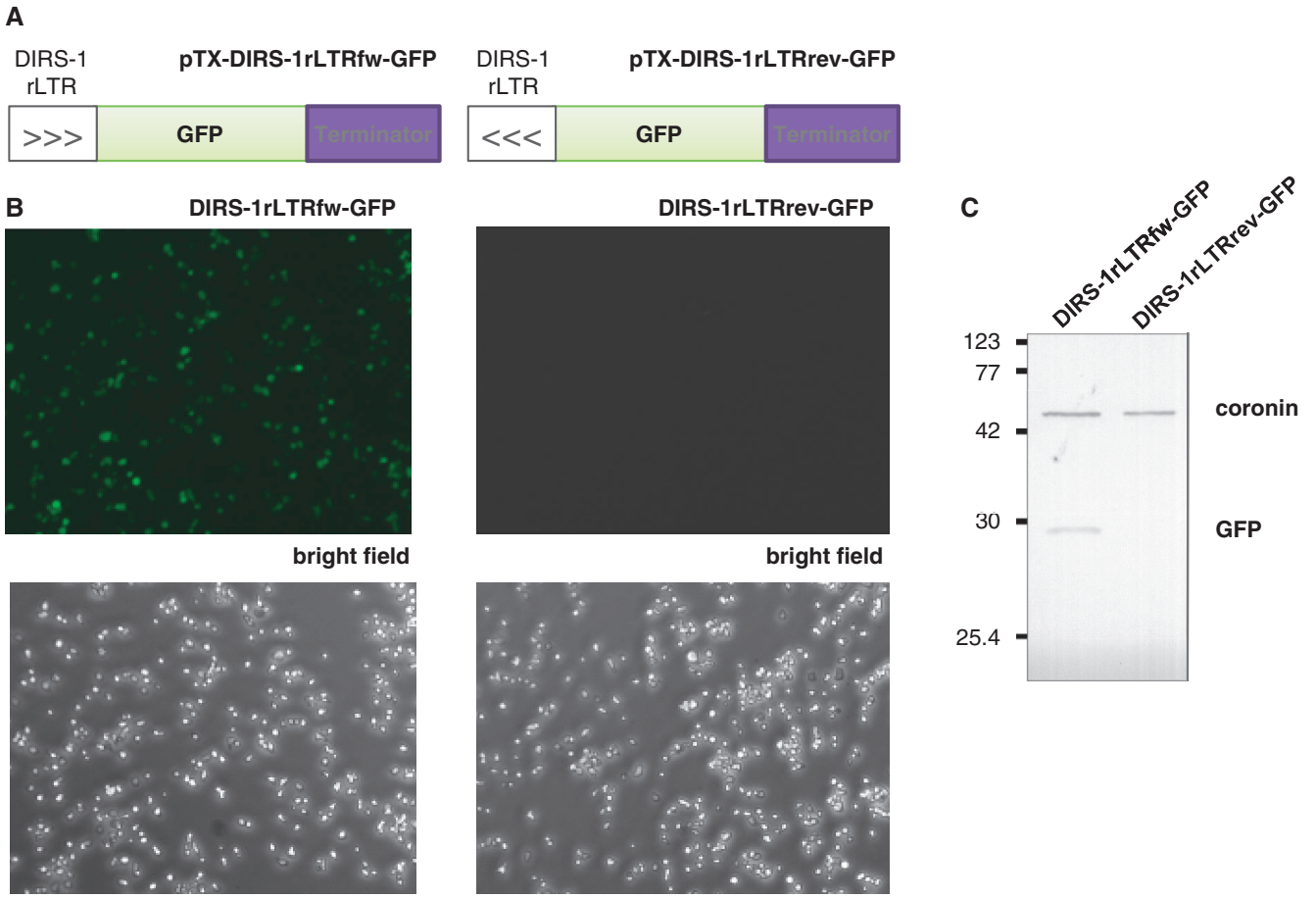

Figure 2. Analysis of DIRS-1 right LTR promoter activity. (**A**) Constructs with forward and reverse right LTR, a GFP ORF and terminator sequence. (**B**) Fluorescence (top) and bright field (bottom) microscopy of AX2 cells transformed with constructs shown in (A). (**C**) Western blot of these transformed cells using antibodies against GFP and Coronin (loading control). The molecular weights of a size marker (in kDa) are indicated to the left.

DIRS-1 transcripts cluster in the nucleus of *rrpC*¯ cells

To determine the localization of DIRS-1 transcripts in amoeba cells, we used a recently established protocol for RNA-FISH in *D. discoideum* (29). First, we generated digoxigenin-labeled strand-specific 500-nt-long probes starting at the LE position of DIRS-1 (Figure 1A), which we used in hybridization experiments of fixed and permeabilized AX2 wild-type and *rrpC*¯ cells. Fluorescence microscopy revealed for either probe diffuse signals that predominantly localized to the cytoplasm in AX2 wild-type cells, as judged from the DAPI staining of the nucleus (Figure 3A). In the *rrpC*¯ strain,

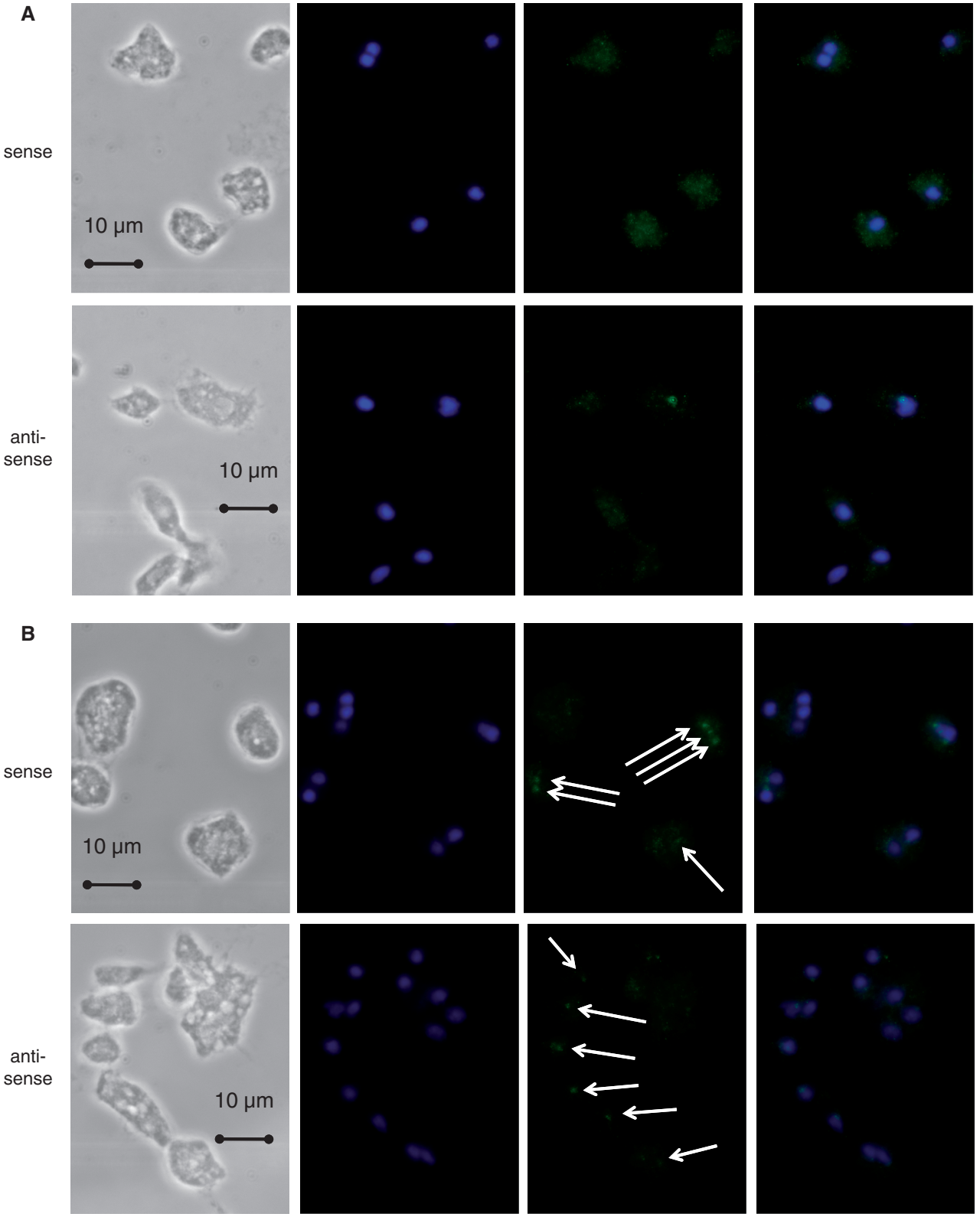

Figure 3. Localization of DIRS-1 transcripts in *D. discoideum* cells by FISH. Sense and antisense DIRS-1 transcripts in AX2 (**A**) and *rrpC*$^{-}$ cells (**B**). Shown are microscopic images of fixed and permeabilized cells. First column: phase contrast; second column: DAPI staining; third column: Alexa Fluor 488-coupled secondary antibody staining of DIRS-1 transcripts; and fourth column: merge of DAPI and Alexa Fluor 488-coupled secondary antibody staining. Arrows mark accumulated transcripts. All pictures were taken at a 100-fold magnification, and a scale bar is indicated for each row in the phase contrast panel. Pictures were taken with exposure times of 260–350 ms for DAPI and 700–1000 ms for Alexa.

additional strong signals were observed (Figure 3B), which appeared to cluster in one or more spots in the nucleus. These clusters of DIRS-1 transcripts were observed by using either the sense or the antisense probe in the *rrpC*$^{-}$ strain (Figure 3B).

As summarized in Table 1, our data indicate that full-length as well as shorter sense DIRS-1 RNAs accumulates in *rrpC*$^{-}$ strains. A long antisense RNA, lasDIRS-1, is also expressed and likely driven by the promoter activity of the right LTR. Shorter fragments of lasDIRS-1 were found to accumulate in the *rrpC*$^{-}$ strains. Compared with the AX2 wild-type strain, additional signals for DIRS-1 sense and antisense transcripts appeared to localize in nuclear spots in the *rrpC*$^{-}$ strain.

DIRS-1-specific small RNAs

Because gene silencing by RdRPs is commonly associated with the appearance of small RNAs, we next analyzed the presence of DIRS-1-specific small RNAs by northern blotting. Using a radioactively labeled oligonucleotide corresponding to the LE position of the retrotransposon, we observed a significant reduction of DIRS-1-specific small RNAs in all strains lacking the *rrpC* gene as compared with the wild-type (Figure 4A). The reduction is also apparent, albeit to a lesser extent, in a northern blot using a probe against the RE position of DIRS-1 (Figure 4B). The individual deletions of the other *rrp* genes, *rrpA* or *rrpB* appeared to have no significant effect on the accumulation of these DIRS-1 small RNAs, and the same is observed for DrnB (Figure 4).

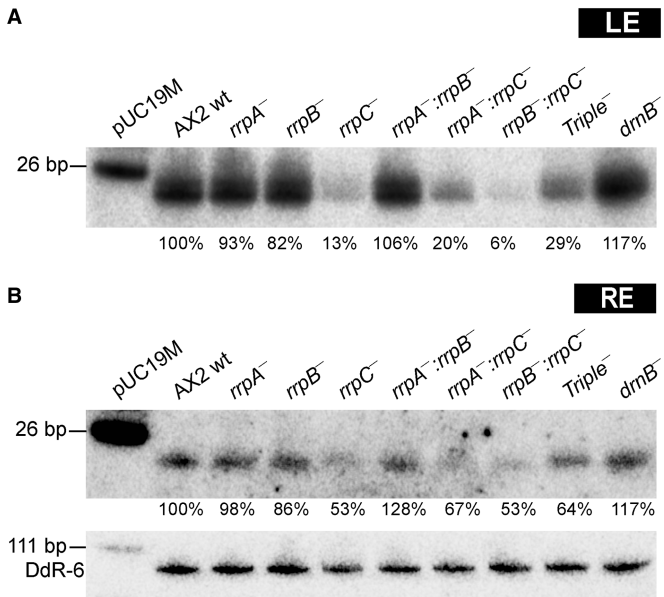

Figure 4. DIRS-1-specific small RNAs expression. Northern blots monitoring the small RNAs of DIRS-1 in the indicated strains, using oligoprobes LE (**A**) or RE (**B**), which are localized to DIRS-1 as indicated in Figure 1A. Quantification of small RNA levels (indicated below the blots) is relative to that of the AX2 wild-type and normalized to the DdR-6 snoRNA sequence (42). The 26-bp band of the size marker pUC19 DNA/*Msp* I is indicated. Northern blot conditions are listed in Supplementary Table S4.

However, with both probes, the decrease appeared less pronounced in the triple knockout strain (see also Table 1), an observation that we cannot explain at present. Yet, these northern blot data indicate that the RdRP RrpC is required for the generation of DIRS-1 small RNAs, at least at the positions LE and RE (Figure 1A). In our previous study, we had observed small RNAs distributed over the entire sequence of the retrotransposon (21). To analyze whether all these DIRS-1 small RNAs depend on RrpC, we next carried out deep sequencing studies on RNA from *D. discoideum* AX2 wild-type and *rrpC*$^{-}$ cells.

Asymmetric distribution of small RNAs over the DIRS-1 sequence

The small RNA profiles of AX2 wild-type and *rrpC*$^{-}$ strains were determined by deep sequencing on an Illumina platform using two biological replicates per strain. This resulted in ~28 and ~16 million sequence reads of 21 nt for AX2 and *rrpC*$^{-}$, respectively. These reads were mapped against the *D. discoideum* genome and a library of repeat sequences (manuscript in preparation).

In the wild-type AX2 strain, a substantial fraction of small RNA sequencing reads (19.5%) corresponded to DIRS-1 sequences, confirming our earlier studies that used 5′-ligation-dependent cloning and SOLiD sequencing of small RNAs from the AX4 strain (43). However, in the *rrpC*$^{-}$ strain, the number of DIRS-1 sequencing reads is strongly (−65%) reduced from 5.5 to 1.9 M, indicating that RrpC might be involved in their generation. We next mapped these small RNA reads on the DIRS-1 sequence (Figure 5A). The comparison of the small RNA distribution patterns in the two biological replicates of the wild-type AX2 strain (Figure 5B) indicates that the data are highly reproducible, and the same holds for the two biological replicates of the *rrpC*$^{-}$ strain (Figure 5C).

The distribution of small RNAs over the DIRS-1 sequence appears uneven in the AX2 strain. The majority of reads coincide with ORF II, while the 5′-end of GAG appears to be devoid of any small RNAs (Figure 5B). This analysis also showed the reduction of the small DIRS-1 RNAs in the *rrpC*$^{-}$ strain, but additionally indicated that not all positions within the retrotransposon are equally affected (Figure 5C). For example, although reduced reads are observed for the majority of DIRS-1 positions in the *rrpC*$^{-}$ strain, this is not the case for the relatively small number of reads that map to the LTRs of the retrotransposon (box I, Figure 5B and C). These LTR-specific small RNAs appear to be unchanged in number and position and thus likely are independent of RrpC. A small number of reads corresponding to the 5′-end of GAG was surprisingly observed only in the *rrpC*$^{-}$ strain, but not in the AX2 wild-type (box II, Figure 5B and C). These small RNAs thus seem to disappear when RrpC is present. Reads mapping around the 3′-end of ORF I and the 5′-end of ORF II appear to be particularly reduced in the *rrpC*$^{-}$ strain (box III, Figure 4B and C), while the distribution of the majority of small RNAs in the *rrpC*$^{-}$ strain has an overall similar

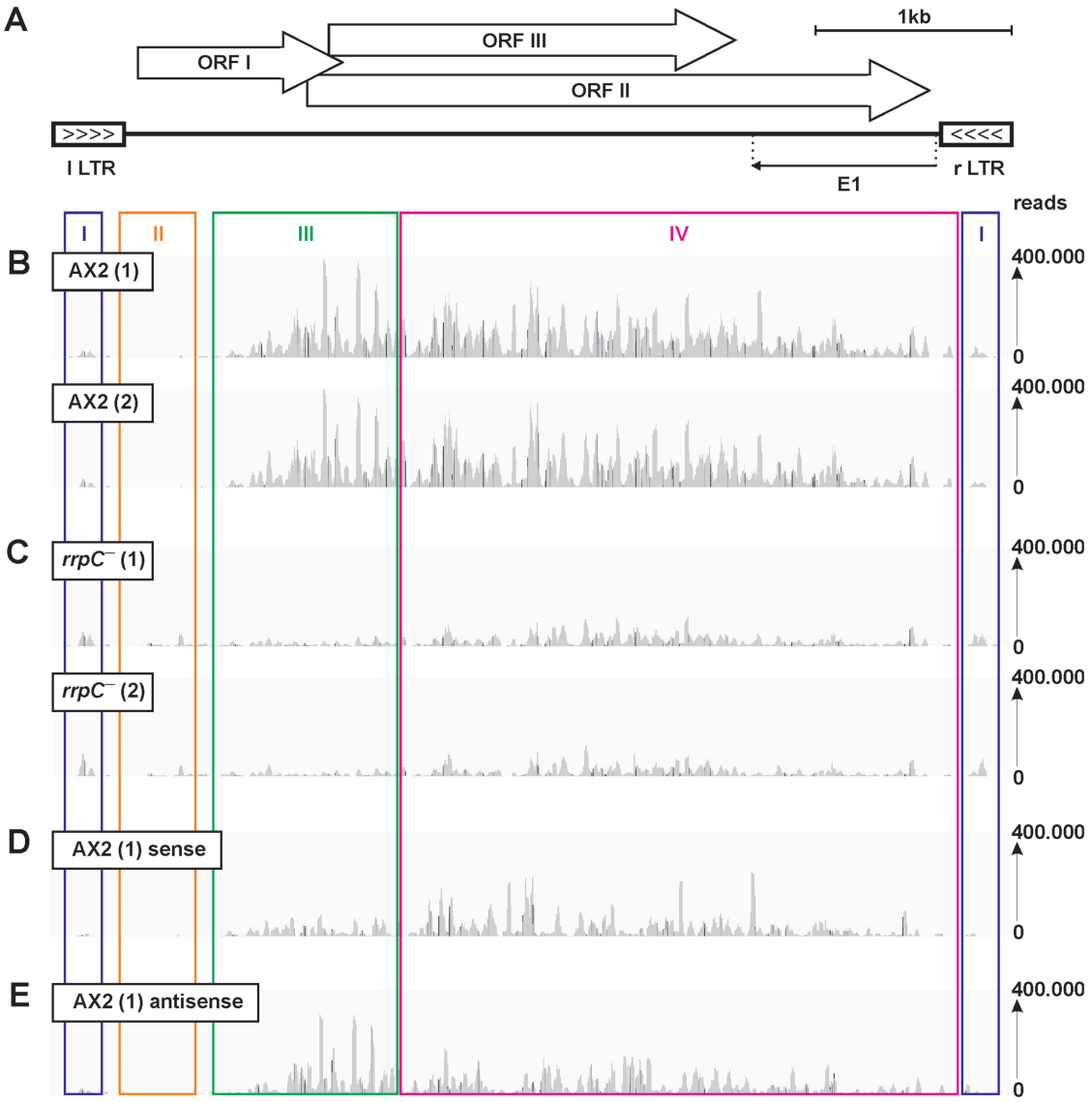

Figure 5. Distribution of DIRS-1-specific small RNAs. (**A**) Schematic representation of the DIRS-1 sequence (for details see Figure 1A). Small RNA reads from the wild-type AX2 strain (**B**) and the *rrpC*⁻ strain (**C**) are shown for their biological duplicates (1 or 2, respectively). The DIRS-1 small RNAs of sample (1) are shown separately for sense (**D**) and antisense (**E**) orientations. All reads are mapped onto the DIRS-1 sequence in (A). The signal height corresponds to the number of small RNAs, and reads are displayed in the same scale, ranging from 0 to 400.000 reads. Regions with particularly apparent deviations between the AX2 and *rrpC*⁻ strains are boxed (I, II, III, IV).

pattern to that observed in the AX2 wild-type strain, albeit at drastically reduced numbers (box IV, Figure 5B and C). These observations suggest that both of these classes of DIRS-1 small RNAs depend on RrpC.

Asymmetric distribution of DIRS-1 small RNAs in sense and antisense orientation

In view of the presence of the lasDIRS-1 transcript (Figures 1D and 3), we next analyzed whether the DIRS-1-specific small RNAs mapped equally in sense and antisense orientation to the retrotransposon. The results showed uneven distribution of the small RNAs, with the sense small RNAs mapping predominantly to ORF II and the antisense RNAs appearing to peak in the region box III (Figure 5D and E). The asymmetry of sense and antisense read distribution indicates that the majority of small DIRS-1 RNAs might not be generated as classical double-stranded siRNAs.

Post-transcriptional silencing of DIRS-1 mRNAs

Because the small DIRS-1 RNAs appear to be unevenly distributed along the three ORFs of the retrotransposon, we wondered what effect they might have on these three ORFs. To investigate this question, we generated over-expression constructs, in which GFP was C-terminally fused to the full mRNA of either ORF (Supplementary Figure S3). The resulting extrachromosomal vector constructs were transformed in the AX2 wild-type and the

rrpC^{-} strain. Expression of the fusion proteins was monitored by western blotting using a GFP antibody. The ORF I-GFP fusion protein was readily expressed in both strains, while expression of the other two ORFs was not detectable in the AX2 wild-type, but notably observed in the *rrpC*$^{-}$ strain (Figure 6A and B). This indicates that the RrpC-dependent small RNAs that are present in the AX2 wild-type strain are necessary and

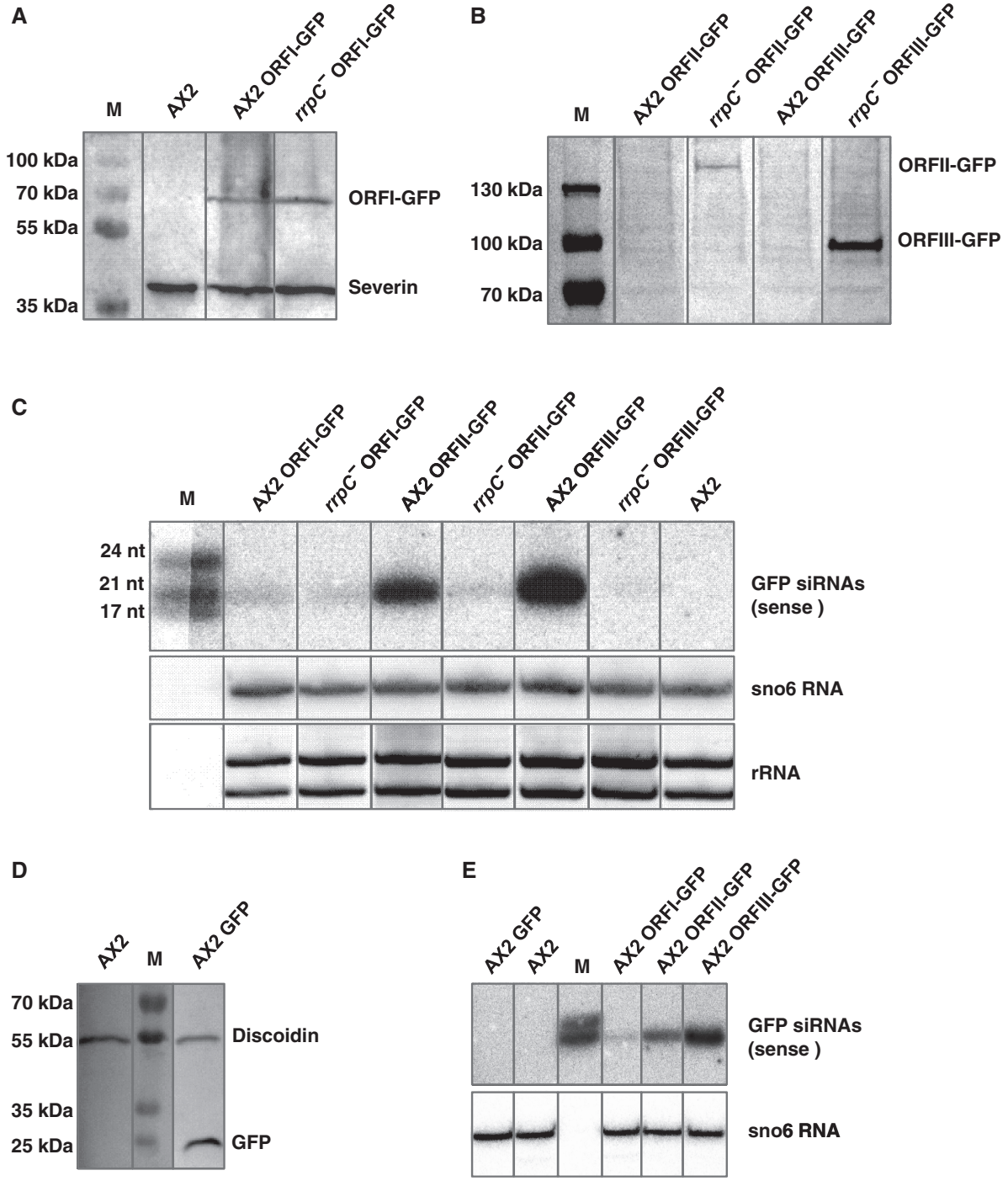

Figure 6. Overexpression of DIRS-1 ORFs. C-terminal GFP fusions of DIRS-1 ORF I (**A**) and ORF II or ORF III (**B**) were expressed in the AX2 wild-type and in the *rrpC*$^{-}$ strain. The expression of the fusion proteins was monitored by western blotting using a GFP antibody (see also Supplementary Figure S3). (**C**) Small GFP RNAs from the indicated strains were analyzed by northern blot using a strand-specific radioactively labeled probe. The sizes of a radioactively labeled RNA size marker are shown to the left. Ethidium bromide-stained rRNA served as loading control, and northern blots using a sno6 riboprobe acted to monitor transfer efficiency. (**D**) Expression of GFP in AX2 wild-type cells. (**E**) Small GFP RNAs from the indicated strains. In (**A**, **B** and **D**), severin or discoidin were used as loading controls, and the sizes of a protein marker are shown. M in (**C** and **E**) denotes small RNA size markers. Northern blot conditions are listed in Supplementary Table S4. Note that boxed lanes are spliced together from the same blot deleting irrelevant samples.

sufficient to silence post-transcriptionally ORF II and ORF III, but not ORF I, of the retrotransposon, even though siRNAs in the 3′ half of ORF I are mostly antisense to the coding transcript and could readily abolish it.

Spreading of the RNA silencing signal in the 3′ direction on the target mRNA

We have recently shown that RrpC is required for the appearance of small RNAs 5′ of the original silencing signal with respect to the target RNA (9). This phenomenon is generally referred to as transitive silencing (6–8), and it is thought that the target RNA serves as the template, from which an RdRP synthesizes a complementary RNA strand. Because of the directionality of all nucleic acid polymerases, such a secondary silencing signal is expected to localize 5′ of the original trigger. However, Pak and Fire reported that a subset of secondary RNAs could also localize 3′ of the original trigger in *C. elegans* (44), an observation that otherwise is mainly seen in the plant kingdom (7,8,45,46). To test whether 3′ spreading might also be observed in the case of the DIRS-1 ORF-GFP fusion constructs, we isolated small RNAs from these strains and used northern blot analysis to identify small RNAs derived from GFP (Figure 6C). Substantial amounts of small GFP-specific sense RNAs were detected in the ORF II-GFP and ORF III-GFP expressing cells in the AX2 wild-type background, but not in the *rrpC*¯ strain. To show that GFP itself does not cause the generation of siRNAs, we transformed the AX2 wild-type with a GFP expression construct alone, which resulted in GFP expressing cells (Figure 6D) and did not cause generation of small GFP RNAs as monitored by northern blotting (Figure 6E). The inclusion of RNA from the C-terminal GFP fusions of the DIRS-1 ORFs serves here as control for the functionality of the blot, as it otherwise would appear empty. Because the GFP was fused C-terminally to the DIRS-1 ORFs, this result indicates that spreading of an RNA silencing signal in the 3′ direction exists in *D. discoideum* and depends on the presence of RrpC (summarized in Table 1). We note that a weak signal for small GFP RNAs is also present in strains where the fusion protein is not silenced, but not in the untransformed AX2 wild-type strain (Figure 6).

Mobilization of DIRS-1 in the genome of the *rrpC*¯ strain

Having shown with the ORF–GFP fusions that DIRS-1 mRNAs are translated in the *rrpC*¯ strain, we next set out to analyze what effects this has on the genome of the *rrpC*¯ strain. However, the genome-wide analysis of DIRS-1 elements is hampered by the large number of DIRS-1 elements and fragments (12) and the fact that DIRS-1 retrotransposition takes place preferentially in other DIRS-1 elements or fragments (15).

To investigate whether new DIRS-1 integrations can be observed in the genome of the *rrpC*¯ strain, we subjected *rrpC*¯ and AX2 wild-type strains to extensive growth for 48 days in shaking cultures kept in the exponential growth phase by regular dilution. Under such conditions, we had earlier observed increased genomic copy numbers of Skipper, when that retrotransposon was dysregulated in a gene deletion strain of the putative DNA methyltransferase DnmA (21). From the AX2 and *rrpC*¯ long-term cultures, genomic DNA was isolated and digested with three different restriction enzymes of which *Eco* RI and *Kpn* I cleave inside the DIRS-1 DNA (Figure 7A), whereas *Sac* I cleaves outside. The restriction patterns of genomic DNA from these two strains appeared to be highly similar (Figure 7B). In the subsequently performed Southern blot (Figure 7C), the overall picture is also similar, as might be expected given the many genomic occurrences of DIRS-1 elements. For the *Eco* RI and the *Sac* I digests, the most prominent signals from the AX2 strain appear to be more intense in the *rrpC*¯ strain genomic DNA, which may indicate an increase in DIRS-1 copy number. More importantly, we observe an additional signal at ∼5 kb in the *rrpC*¯ strain in the *Kpn* I digest, clearly indicating a DIRS-1 retrotransposition event (Figure 7C). To quantify these differences in DIRS-1 copy number, Southern blotting was repeated and signals for DIRS-1 and the thioredoxin gene as loading control were quantified for two digests of genomic DNA from AX2 wild-type and the *rrpC*¯ strain (Supplementary Table S5). This analysis confirmed an increase in DIRS-1 copy numbers by >50% in the *rrpC*¯ strain compared with the AX2 wild-type, as shown by loading-corrected signal increases of 52% and 62% for the two restriction enzymes used (Supplementary Table S5). Together, the data indicate that additional genomic copies of the retrotransposon accumulate in the genome of the *rrpC*¯ strain. This is further supported by a previous analysis of DIRS-1 copy numbers in the originally generated gene disruption strain of the *rrpC* gene (21), where different DIRS-1 patterns were observed in clonal long-term cultures (M. Kuhlmann and W. Nellen, unpublished).

DISCUSSION

In the present study, we show that the RdRP RrpC acts in the regulation of the centromeric retrotransposon DIRS-1. We report that sense transcripts accumulate in strains lacking the *rrpC* gene (Figure 1; summarized in Figure 8) and concurrent with this accumulation, DIRS-1-specific small RNAs are dramatically reduced (Figures 4 and 5; summarized in Table 1). As a consequence of their absence, it is likely that the DIRS-1 ORFs II and III are no longer silenced, leading to the accumulation of DIRS-1 proteins as monitored by GFP fusions (Figure 6) and DIRS-1 retrotransposition (Figure 7) in the *rrpC*¯ cells. From these data, we propose that DIRS-1 is constitutively transcribed in wild-type cells, and these transcripts are targeted by RrpC, which thus exerts it control predominantly on the post-transcriptional level.

For the full-length DIRS-1 elements, transcription is driven by the inherent promoter activity of the two LTRs, as reported earlier for the left LTR (18) and in this study for the right LTR (Figure 2), resulting in the newly discovered lncRNA antisense transcript lasDIRS-1 (Figure 1). The observation that the full-length lasDIRS-1

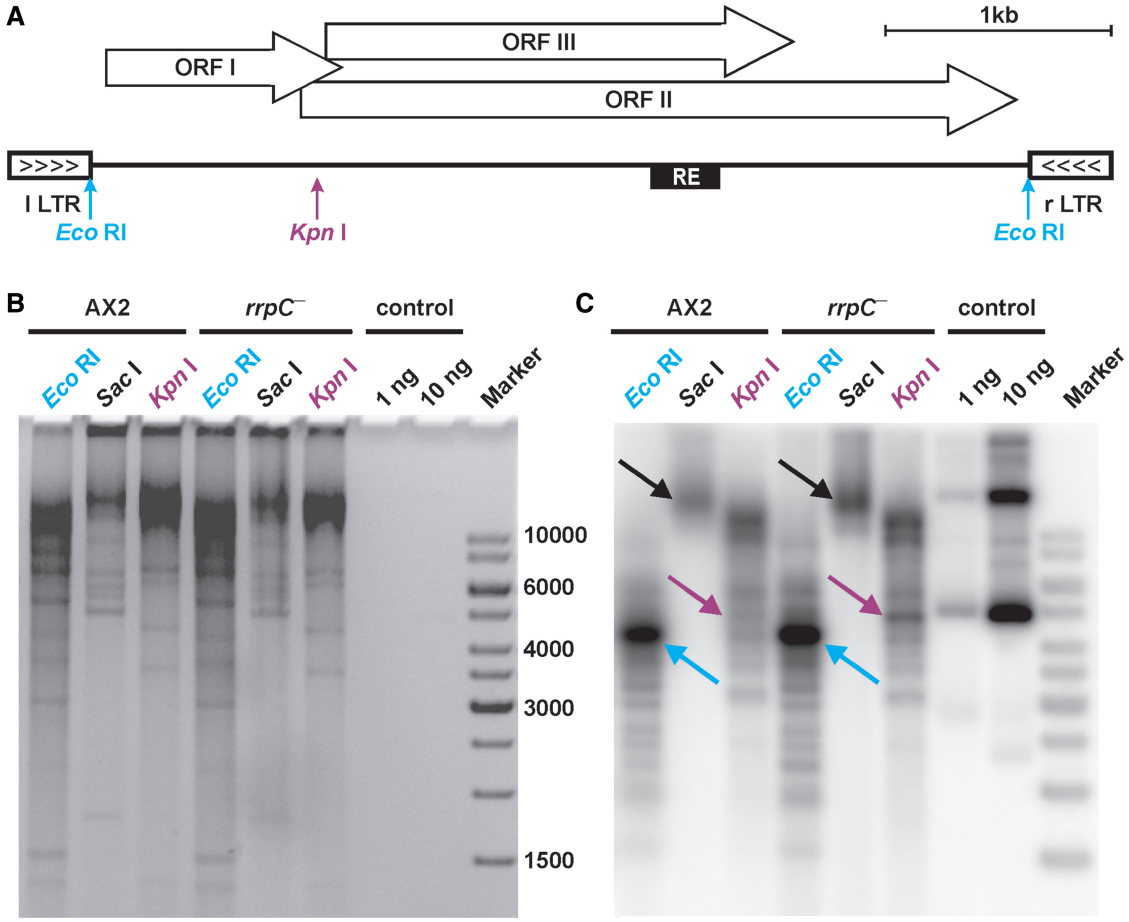

Figure 7. Southern blot analysis for genomic mobilization of DIRS-1 in the *rrpC*⁻ strain. (**A**) Schematic representation of DIRS-1 with recognition sites of *Eco* RI and *Kpn* I that cleave within the retrotransposon sequence, while *Sac* I (not shown) does not. (**B**) Agarose gel electrophoresis of 20 µg genomic DNA from AX2 wild-type and *rrpC*⁻ strains, digested with the indicated restriction endonucleases. As controls for hybridization, 1 or 10 ng undigested plasmid DNA featuring the DIRS-1 sequence was applied. The sizes of the 1-kb marker fragments (ThermoScientific) are indicated. (**C**) Southern blot using a ^{32}P-labeled DNA probe corresponding to the RE position. Note that the positions with an additional or stronger signals observed for the *rrpC*⁻ genomic DNA are indicated by arrows using the same colors for *Eco* RI and *Kpn* I as in (A). Changes in patterns of DNA digested with *Sac* I, which cleaves outside DIRS-1, are denoted by black arrows.

transcript is also present in the triple *rrp* gene deletion strain excludes the possibility that it might be an RdRP product. The sense and antisense transcripts that result from the LTR promoter activities appear to have different fates in the investigated cell lines. The levels of the lncRNA lasDIRS-1 are stable, whereas those of the sense RNA vary significantly (Figure 1; summarized in Figure 8). In particular, we observe a dramatic accumulation of full-length and shorter DIRS-1 sense transcripts, next to shorter versions of the lasDIRS-1 lncRNA in all deletion strains of the *rrpC* gene (Figure 1). As shown by RNA FISH, additional DIRS-1 signals can be observed in the nucleus of *rrpC*⁻ cells (Figure 3), and it appears plausible that the accumulating shorter sense and antisense transcripts that we observe by northern blotting are contained in these spots. Bidirectional transcription has also been observed for retrotransposons in other organisms, including LINE-1 in humans (47); LINE elements, SINE elements and LTR retrotransposons in mice (48,49); Tc1 in *C. elegans* (50); and transposons in *Drosophila* (51,52).

Concurrent with the accumulation of long transcripts, we observe by northern blot analyses and by deep sequencing (Figures 4 and 5), a drastic reduction of small DIRS-1 RNAs in strains lacking the *rrpC* gene. In the deep sequencing analysis, we find the majority of small RNAs to be asymmetrically distributed between the sense and antisense orientations of the retroelement in AX2 cells. This result indicates that these small RNAs are not reaction products of one of the two Dicer-like proteins in *D. discoideum* (21,39,43), because Dicers are expected to give rise to double-stranded siRNAs (53–55), which should cover DIRS-1 symmetrically in sense and antisense orientation.

Because the majority of small DIRS-1 RNAs disappear in the absence of RrpC, the simplest explanation is that these are directly synthesized by this RdRP. The synthesis of small RNAs by RdRPs has also been described in other species, including *C. elegans* (44,56), *Neurospora crassa* (57) and *Arabidopsis thaliana* (58). Our conclusion is also in line with our recently reported discovery that RrpC is required for the 5′ spreading of an RNA silencing

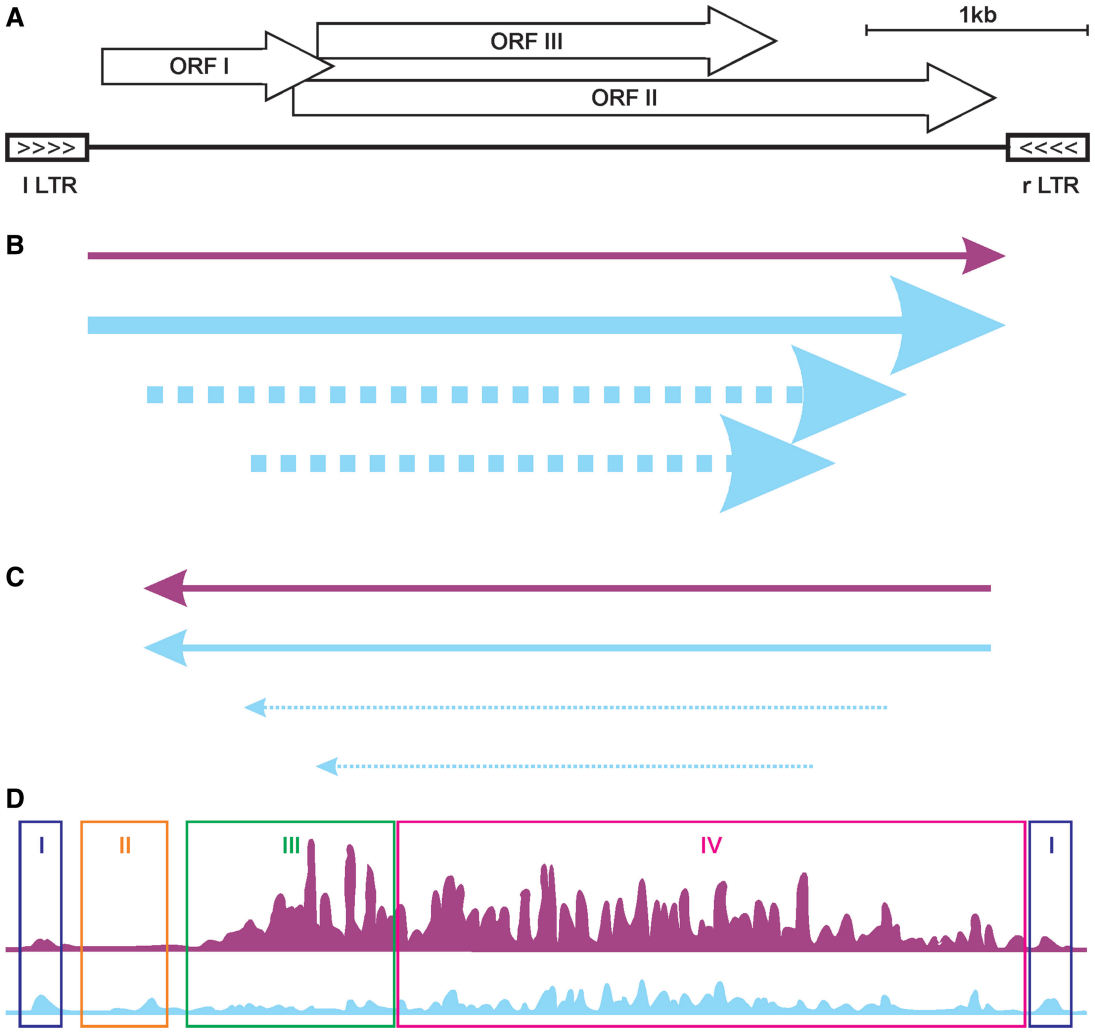

Figure 8. Summary of DIRS-1 RNAs in AX2 and *rrpC*$^{-}$ strains. (**A**) Schematic representation of the DIRS-1 sequence (for details see Figure 1A). Relative levels of DIRS-1 sense transcripts (**B**), antisense transcripts (**C**) and small RNAs (**D**) are shown for the AX2 wild-type (purple) and for the *rrpC*$^{-}$ (light blue) strains. Arrows in (B) and (C) represent the transcripts mapped onto the DIRS-1 element in (A). The thickness of the arrows indicates relative changes in RNA quantity. Note that RNA levels are comparable only within panels and that the positions of the shorter fragments (dotted) are not exactly determined. In (D), the distribution of small RNAs is also mapped onto the element in (A) and the height of the peaks indicates abundance, using the same relative scaling (for details see Figure 5).

signal (9). Changes in the distribution of small DIRS-1 RNAs in the *rrpC*$^{-}$ strain compared with AX2 appear to cluster in four regions (boxes I-IV in Figure 5; summarized in Figure 8), which correspond to the LTR with unchanged levels (I), to the 5′-end of GAG with small RNAs absent in AX2 (II), to a region with barely any small RNAs left (III) and to a region with reduced numbers but a similar distribution pattern (IV). For the latter, RrpC might serve as the amplifying component of a primary silencing signal, like a double-stranded RNA. Such an entity has been proposed earlier by Fire and Mello, when they discovered RNAi in *C. elegans* (4). The responsible enzyme was characterized subsequently as the RdRP EGO-1 (5). The small RNAs in region III appear to strongly accumulate in antisense orientation (Figure 5E). We propose that RrpC synthesizes these small RNAs, using the DIRS-1 sense transcript as a template. Why these RNA appear to be non-functional in the post-transcriptional silencing of the ORF I-GFP fusion protein (Figure 6A) is currently unclear, but one possible reason is that their concentration in that region might be too low (Figure 5).

The small RNAs of the LTR region, on the other hand, appear to be unaffected by the deletion of *rrpC*, and in view of their symmetric sense and antisense distribution, they might represent Dicer products. In this respect, it is worth noting that the sense transcript has been shown to contain little of the left LTR, but nearly the entire right LTR (18). Of these expressed right and left LTR sequences, 58 nt and 33 nt, respectively, are complementary to a DIRS-1 region termed the ICR. During DIRS-1 retrotransposition, the ICR is proposed to bring the 5′-end and the 3′-end of a reverse transcript together (11), to allow for the formation of a single-stranded circular DNA replication intermediate (17). It seems plausible to suggest that such base pairing also takes

place on the RNA level, and the resulting RNA double strands would be long enough to allow for Dicer activity, giving rise to the RrpC-independent DIRS-1 LTR siRNAs (box I in Figures 5 and 8).

Although the small DIRS-1 RNAs that are present only in the absence of RrpC (box II, Figures 5 and 8) are low in number, they appear reproducibly. Similarly, elevated small RNA levels in strains lacking the functional *rrpC* gene have also been shown for endogenous microRNAs (39,43), the retrotransposon Skipper (43), and recently also in transgene silencing (9). Given that RdRPs are enzymes that synthesize RNA, small RNA accumulation in their absence is counter-intuitive. However, some RdRPs in other organisms (57,58) have been proposed to act in a small RNA primer-dependent mode, in which the RNA primer is extended, resulting in the formation of long double-stranded RNAs, which act as *bona fide* Dicer substrates. If primer extension does not take place, the primers might accumulate. In view of small RNAs from various genetic backgrounds accumulating in *rrpC*$^{-}$ strains, a primer-dependent activity of this RdRP on these sequences appears to be a plausible interpretation. Albeit indirectly, this interpretation is also supported by the observation that classical (3′–5′) transitive silencing in *D. discoideum* depends on both, the dicer-related nuclease DrnB and RrpC (9). Also for several other RdRPs, both primer-dependent and -independent modes of action have been inferred, like QDE-1 in *N. crassa* (57) or the *A. thaliana* enzyme RDR6 (58,59), which act in the primer-dependent mode also in the biosynthesis of tasiRNAs (58,60).

To our surprise, we observed significant levels of small RNAs 3′ to the endogenous DIRS-1 small RNA trigger during the analysis of the C-terminal GFP fusion constructs of the DIRS-1 ORFs (Figure 6). Substantial amounts of GFP-specific small RNAs were only detectable for the ORF II and ORF III fusion constructs, but not for ORF I-GFP. Early work on the activity of RdRPs has shown that unprimed activity is preferentially observed at the 3′-end of mRNAs (61,62). Because the small GFP RNAs are not observed in the GAG–GFP construct, it appears unlikely that the GFP mRNA sequence itself is recognized as aberrant and is causative for the observed spreading in the 3′ direction. Because the presence of GFP alone does not lead to the generation of small GFP RNAs (Figures 2 and 6D and E), this possibility can be excluded. From the use of probes monitoring small GFP RNAs in the sense orientation, we conclude that these are not direct products of RrpC on the mRNA of the respective ORF–GFP. Rather, they are likely processing products of an RrpC-dependant double-strand that might be targeted by one of the *D. discoideum* Argonaute or Dicer proteins.

In a previous study, we had investigated transcriptional silencing of DIRS-1 by DNA methylation. Although the DIRS-1 right LTR was found to be methylated by the sole DNA methyltransferase in *D. discoideum*, DnmA (21), a deletion of its gene did not result in a transcriptional upregulation of DIRS-1. From this, we concluded that DIRS-1 is not under transcriptional control by DnmA, unlike the retrotransposon Skipper (21). However, we cannot exclude the possibility that other components of the heterochromatization machineries in the amoeba might add a transcriptional control of DIRS-1 in addition to the post-transcriptional control by RrpC that we report here.

Control at the post-transcriptional level appears uneconomic, as DIRS-1 transcripts are first generated in order to then be degraded. However, this control might be a consequence of the integration behavior of DIRS-1. Because DIRS-1 retrotransposition takes place preferentially into other DIRS-1 elements or fragments thereof (15), highly diverse DIRS-1 sequences are expected to be produced. In these diverse DIRS-1 sequences, motifs other than the LTRs might serve as promoters, which then might render the mobile genetic elements refractory to transcriptional control, at least by using LTR promoter methylation.

SUPPLEMENTARY DATA

Supplementary Data are available at NAR Online.

ACKNOWLEDGEMENTS

The authors thank Dianna K. Bautista and Timothy J. Wilson for most helpful comments on the manuscript. The authors acknowledge support from Science for Life Laboratory, the National Genomics Infrastructure (NGI) and Uppmax for providing assistance in massively parallel sequencing and computational infrastructure. They also thank Markus Maniak for providing antibodies against GFP, Severin and Coronin.

FUNDING

The Deutsche Forschungsgemeinschaft [Heisenberg stipend HA3459/5-2, HA3459/7-1 to C.H., Wi1142/6-1 to T.W.]; by the European Molecular Biology Organisation [ASTF497-2011 to C.S.] and by the Swedish Research Council [to O.E. and F.S.]; Supported by a stipend from the Land Hessen (to D.M. and B.B.). Funding for open access charge: Deutsche Forschungsgemeinschaft.

Conflict of interest statement. None declared.

REFERENCES

1. Maida,Y., Yasukawa,M., Furuuchi,M., Lassmann,T., Possemato,R., Okamoto,N., Kasim,V., Hayashizaki,Y., Hahn,W.C. and Masutomi,K. (2009) An RNA-dependent RNA polymerase formed by TERT and the RMRP RNA. *Nature*, **461**, 230–235.
2. Maida,Y. and Masutomi,K. (2011) RNA-dependent RNA polymerases in RNA silencing. *Biol. Chem.*, **392**, 299–304.
3. Wassenegger,M. and Krczal,G. (2006) Nomenclature and functions of RNA-directed RNA polymerases. *Trends Plant Sci.*, **11**, 142–151.
4. Fire,A., Xu,S., Montgomery,M.K., Kostas,S.A., Driver,S.E. and Mello,C.C. (1998) Potent and specific genetic interference by double-stranded RNA in *Caenorhabditis elegans*. *Nature*, **391**, 806–811.

5. Smardon,A., Spoerke,J.M., Stacey,S.C., Klein,M.E., Mackin,N. and Maine,E.M. (2000) EGO-1 is related to RNA-directed RNA polymerase and functions in germ-line development and RNA interference in *C. elegans*. *Curr. Biol.*, **10**, 169–178.
6. Sijen,T., Fleenor,J., Simmer,F., Thijssen,K.L., Parrish,S., Timmons,L., Plasterk,R.H. and Fire,A. (2001) On the role of RNA amplification in dsRNA-triggered gene silencing. *Cell*, **107**, 465–476.
7. Vaistij,F.E., Jones,L. and Baulcombe,D.C. (2002) Spreading of RNA targeting and DNA methylation in RNA silencing requires transcription of the target gene and a putative RNA-dependent RNA polymerase. *Plant Cell*, **14**, 857–867.
8. Voinnet,O., Vain,P., Angell,S. and Baulcombe,D.C. (1998) Systemic spread of sequence-specific transgene RNA degradation in plants is initiated by localized introduction of ectopic promoterless DNA. *Cell*, **95**, 177–187.
9. Wiegand,S. and Hammann,C. (2013) The 5′ spreading of small RNAs in *Dictyostelium discoideum* depends on the RNA-dependent RNA polymerase RrpC and on the dicer-related nuclease DrnB. *PLoS One*, **8**, e64804.
10. Martens,H., Novotny,J., Oberstrass,J., Steck,T.L., Postlethwait,P. and Nellen,W. (2002) RNAi in Dictyostelium: the role of RNA-directed RNA polymerases and double-stranded RNase. *Mol. Biol. Cell*, **13**, 445–453.
11. Poulter,R.T. and Goodwin,T.J. (2005) DIRS-1 and the other tyrosine recombinase retrotransposons. *Cytogenet. Genome Res.*, **110**, 575–588.
12. Eichinger,L., Pachebat,J.A., Glöckner,G., Rajandream,M.A., Sucgang,R., Berriman,M., Song,J., Olsen,R., Szafranski,K., Xu,Q. *et al.* (2005) The genome of the social amoeba *Dictyostelium discoideum*. *Nature*, **435**, 43–57.
13. Dubin,M., Fuchs,J., Graf,R., Schubert,I. and Nellen,W. (2010) Dynamics of a novel centromeric histone variant CenH3 reveals the evolutionary ancestral timing of centromere biogenesis. *Nucleic Acids Res.*, **38**, 7526–7537.
14. Glöckner,G. and Heidel,A.J. (2009) Centromere sequence and dynamics in *Dictyostelium discoideum*. *Nucleic Acids Res.*, **37**, 1809–1816.
15. Cappello,J., Cohen,S.M. and Lodish,H.F. (1984) *Dictyostelium* transposable element DIRS-1 preferentially inserts into DIRS-1 sequences. *Mol. Cell. Biol.*, **4**, 2207–2213.
16. Winckler,T., Schiefner,J., Spaller,T. and Siol,O. (2011) *Dictyostelium* transfer RNA gene-targeting retrotransposons: studying mobile element-host interactions in a compact genome. *Mob. Genet. Elements*, **1**, 145–150.
17. Cappello,J., Handelsman,K. and Lodish,H.F. (1985) Sequence of *Dictyostelium* DIRS-1: an apparent retrotransposon with inverted terminal repeats and an internal circle junction sequence. *Cell*, **43**, 105–115.
18. Cohen,S.M., Cappello,J. and Lodish,H.F. (1984) Transcription of *Dictyostelium discoideum* transposable element DIRS-1. *Mol. Cell. Biol.*, **4**, 2332–2340.
19. Rosen,E., Sivertsen,A. and Firtel,R.A. (1983) An unusual transposon encoding heat shock inducible and developmentally regulated transcripts in *Dictyostelium*. *Cell*, **35**, 243–251.
20. Zuker,C., Cappello,J., Chisholm,R.L. and Lodish,H.F. (1983) A repetitive *Dictyostelium* gene family that is induced during differentiation and by heat shock. *Cell*, **34**, 997–1005.
21. Kuhlmann,M., Borisova,B.E., Kaller,M., Larsson,P., Stach,D., Na,J., Eichinger,L., Lyko,F., Ambros,V., Söderbom,F. *et al.* (2005) Silencing of retrotransposons in *Dictyostelium* by DNA methylation and RNAi. *Nucleic Acids Res.*, **33**, 6405–6417.
22. Pall,G.S., Codony-Servat,C., Byrne,J., Ritchie,L. and Hamilton,A. (2007) Carbodiimide-mediated cross-linking of RNA to nylon membranes improves the detection of siRNA, miRNA and piRNA by northern blot. *Nucleic Acids Res.*, **35**, e60.
23. Southern,E.M. (1975) Detection of specific sequences among DNA fragments separated by gel electrophoresis. *J. Mol. Biol.*, **98**, 503–517.
24. Hughes,J.E. and Welker,D.L. (1988) A mini-screen technique for analyzing nuclear DNA from a single *Dictyostelium* colony. *Nucleic Acids Res.*, **16**, 2338.
25. Green,M.R. and Sambrook,J. (2012) *Molecular Cloning: a Laboratory Manual*. 4th edn. Cold Spring Harbor Laboratory Press, Cold Spring Harbor, NY.
26. Levi,S., Polyakov,M. and Egelhoff,T.T. (2000) Green fluorescent protein and epitope tag fusion vectors for *Dictyostelium discoideum*. *Plasmid*, **44**, 231–238.
27. Faix,J., Kreppel,L., Shaulsky,G., Schleicher,M. and Kimmel,A.R. (2004) A rapid and efficient method to generate multiple gene disruptions in *Dictyostelium discoideum* using a single selectable marker and the Cre-loxP system. *Nucleic Acids Res.*, **32**, e143.
28. Veltman,D.M., Akar,G., Bosgraaf,L. and Van Haastert,P.J. (2009) A new set of small, extrachromosomal expression vectors for *Dictyostelium discoideum*. *Plasmid*, **61**, 110–118.
29. Hofmann,P., Kruse,J. and Hammann,C. (2013) Transcript localization in *D. discoideum* cells by RNA FISH. *Methods Mol. Biol.*, **983**, 311–323.
30. Bilzer,A., Dolz,H., Reinhardt,A., Schmith,A., Siol,O. and Winckler,T. (2011) The C-module-binding factor supports amplification of TRE5-A retrotransposons in the *Dictyostelium discoideum* genome. *Eukaryot. Cell*, **10**, 81–86.
31. Lucas,J., Bilzer,A., Moll,L., Zundorf,I., Dingermann,T., Eichinger,L., Siol,O. and Winckler,T. (2009) The carboxy-terminal domain of *Dictyostelium* C-module-binding factor is an independent gene regulatory entity. *PLoS One*, **4**, e5012.
32. Pfaffl,M.W. (2001) A new mathematical model for relative quantification in real-time RT-PCR. *Nucleic Acids Res.*, **29**, e45.
33. Hällman,J., Avesson,L., Reimegård,J., Käller,M. and Söderbom,F. (2013) Identificaton and verification of microRNAs by high-throughput sequencing. *Methods Mol. Biol.*, **983**, 125–138.
34. Martin,M. (2011) Cutadapt removes adapter sequences from high-throughput sequencing reads. *EMBnet J.*, **17**, 10–12.
35. Langmead,B., Trapnell,C., Pop,M. and Salzberg,S.L. (2009) Ultrafast and memory-efficient alignment of short DNA sequences to the human genome. *Genome Biol.*, **10**, R25.
36. Jurka,J., Kapitonov,V.V., Pavlicek,A., Klonowski,P., Kohany,O. and Walichiewicz,J. (2005) Repbase Update, a database of eukaryotic repetitive elements. *Cytogenet. Genome Res.*, **110**, 462–467.
37. Robinson,J.T., Thorvaldsdottir,H., Winckler,W., Guttman,M., Lander,E.S., Getz,G. and Mesirov,J.P. (2011) Integrative genomics viewer. *Nat. Biotechnol.*, **29**, 24–26.
38. Wiegand,S., Kruse,J., Gronemann,S. and Hammann,C. (2011) Efficient generation of gene knockout plasmids for *Dictyostelium discoideum* using one-step cloning. *Genomics*, **97**, 321–325.
39. Avesson,L., Reimegard,J., Wagner,E.G. and Söderbom,F. (2012) MicroRNAs in Amoebozoa: deep sequencing of the small RNA population in the social amoeba *Dictyostelium discoideum* reveals developmentally regulated microRNAs. *RNA*, **18**, 1771–1782.
40. Werner,A. (2005) Natural antisense transcripts. *RNA Biol.*, **2**, 53–62.
41. Faghihi,M.A. and Wahlestedt,C. (2009) Regulatory roles of natural antisense transcripts. *Nat. Rev. Mol. Cell Biol.*, **10**, 637–643.
42. Aspegren,A., Hinas,A., Larsson,P., Larsson,A. and Soderbom,F. (2004) Novel non-coding RNAs in *Dictyostelium discoideum* and their expression during development. *Nucleic Acids Res.*, **32**, 4646–4656.
43. Hinas,A., Reimegard,J., Wagner,E.G., Nellen,W., Ambros,V.R. and Soderbom,F. (2007) The small RNA repertoire of Dictyostelium discoideum and its regulation by components of the RNAi pathway. *Nucleic Acids Res.*, **35**, 6714–6726.
44. Pak,J. and Fire,A. (2007) Distinct populations of primary and secondary effectors during RNAi in *C. elegans*. *Science*, **315**, 241–244.
45. Klahre,U., Crete,P., Leuenberger,S.A., Iglesias,V.A. and Meins,F. Jr (2002) High molecular weight RNAs and small interfering RNAs induce systemic posttranscriptional gene silencing in plants. *Proc. Natl Acad. Sci. USA*, **99**, 11981–11986.
46. Braunstein,T.H., Moury,B., Johannessen,M. and Albrechtsen,M. (2002) Specific degradation of 3′ regions of GUS mRNA in posttranscriptionally silenced tobacco lines may be related to 5′-3′ spreading of silencing. *RNA*, **8**, 1034–1044.

47. Yang,N. and Kazazian,H.H. Jr (2006) L1 retrotransposition is suppressed by endogenously encoded small interfering RNAs in human cultured cells. *Nat. Struct. Mol. Biol.*, **13**, 763–771.
48. Watanabe,T., Takeda,A., Tsukiyama,T., Mise,K., Okuno,T., Sasaki,H., Minami,N. and Imai,H. (2006) Identification and characterization of two novel classes of small RNAs in the mouse germline: retrotransposon-derived siRNAs in oocytes and germline small RNAs in testes. *Genes Dev.*, **20**, 1732–1743.
49. Watanabe,T., Totoki,Y., Toyoda,A., Kaneda,M., Kuramochi-Miyagawa,S., Obata,Y., Chiba,H., Kohara,Y., Kono,T., Nakano,T. *et al.* (2008) Endogenous siRNAs from naturally formed dsRNAs regulate transcripts in mouse oocytes. *Nature*, **453**, 539–543.
50. Sijen,T. and Plasterk,R.H. (2003) Transposon silencing in the *Caenorhabditis elegans* germ line by natural RNAi. *Nature*, **426**, 310–314.
51. Chung,W.J., Okamura,K., Martin,R. and Lai,E.C. (2008) Endogenous RNA interference provides a somatic defense against *Drosophila* transposons. *Curr. Biol.*, **18**, 795–802.
52. Ghildiyal,M., Seitz,H., Horwich,M.D., Li,C., Du,T., Lee,S., Xu,J., Kittler,E.L., Zapp,M.L., Weng,Z. *et al.* (2008) Endogenous siRNAs derived from transposons and mRNAs in *Drosophila* somatic cells. *Science*, **320**, 1077–1081.
53. Bernstein,E., Caudy,A.A., Hammond,S.M. and Hannon,G.J. (2001) Role for a bidentate ribonuclease in the initiation step of RNA interference. *Nature*, **409**, 363–366.
54. Ketting,R.F., Fischer,S.E., Bernstein,E., Sijen,T., Hannon,G.J. and Plasterk,R.H. (2001) Dicer functions in RNA interference and in synthesis of small RNA involved in developmental timing in *C. elegans*. *Genes Dev.*, **15**, 2654–2659.
55. Knight,S.W. and Bass,B.L. (2001) A role for the RNase III enzyme DCR-1 in RNA interference and germ line development in *Caenorhabditis elegans*. *Science*, **293**, 2269–2271.
56. Sijen,T., Steiner,F.A., Thijssen,K.L. and Plasterk,R.H. (2007) Secondary siRNAs result from unprimed RNA synthesis and form a distinct class. *Science*, **315**, 244–247.
57. Makeyev,E.V. and Bamford,D.H. (2002) Cellular RNA-dependent RNA polymerase involved in posttranscriptional gene silencing has two distinct activity modes. *Mol. Cell*, **10**, 1417–1427.
58. Moissiard,G., Parizotto,E.A., Himber,C. and Voinnet,O. (2007) Transitivity in *Arabidopsis* can be primed, requires the redundant action of the antiviral Dicer-like 4 and Dicer-like 2, and is compromised by viral-encoded suppressor proteins. *RNA*, **13**, 1268–1278.
59. Curaba,J. and Chen,X. (2008) Biochemical activities of *Arabidopsis* RNA-dependent RNA polymerase 6. *J. Biol. Chem.*, **283**, 3059–3066.
60. Allen,E., Xie,Z., Gustafson,A.M. and Carrington,J.C. (2005) microRNA-directed phasing during trans-acting siRNA biogenesis in plants. *Cell*, **121**, 207–221.
61. Schiebel,W., Haas,B., Marinkovic,S., Klanner,A. and Sanger,H.L. (1993) RNA-directed RNA polymerase from tomato leaves. I. Purification and physical properties. *J. Biol. Chem.*, **268**, 11851–11857.
62. Schiebel,W., Haas,B., Marinkovic,S., Klanner,A. and Sanger,H.L. (1993) RNA-directed RNA polymerase from tomato leaves. II. Catalytic *in vitro* properties. *J. Biol. Chem.*, **268**, 11858–11867.